PAPER

Zn vacancies creation via (2 × 2) surface reconstruction

IOP Publishing Journal of Physics D: Applied Physics
J. Phys. D: Appl. Phys. **50** (2017) 325304 (6pp) https://doi.org/10.1088/1361-6463/aa7b07

Zn vacancies creation via (2 × 2) surface reconstruction

Xiuhua Xie, Binghui Li, Zhenzhong Zhang and Dezhen Shen

State Key Laboratory of Luminescence and Applications, Changchun Institute of Optics, Fine Mechanics and Physics, Chinese Academy of Sciences, Changchun 130033, People's Republic of China

E-mail: binghuili@163.com and shendz@ciomp.ac.cn

Received 10 May 2017, revised 14 June 2017
Accepted for publication 22 June 2017
Published 19 July 2017

Abstract

Zinc vacancies have been incorporated in ZnO via (2 × 2) surface reconstruction during the epitaxy growth. Evolution of *in situ* reflection high-energy electron diffraction (RHEED) patterns indicate Zn-polar surface (2 × 2) reconstruction was realized under extreme O-rich conditions. Atom sized triangular pits and islands were presented by the high resolution scanning tunneling microscopy (STM) images, which stand for a single Zn vacancy per (2 × 2) surface unit cell. The neutral acceptor-bound exciton (A^0,X), peak located at 3.344 eV, and red luminescence (RL), maximum emission intensity at ~1.76 eV, which related to Zn vacancy, have been studied by variable-temperature/power steady-state photoluminescence (PL) spectroscopy.

Keywords: surface reconstruction, Zinc vacancies, Zinc oxide

(Some figures may appear in colour only in the online journal)

1. Introduction

Zinc oxide is one of the attractive candidates of short-wavelength optoelectronic materials, due to its wide band gap of about 3.37 eV and large exciton binding energy (60 meV) [1, 2]. Hitherto, the effective p-type doping represents a crucial challenge for ZnO which is an as-grown n-type conductivity due to native defects and residual impurities [3, 4]. Among published results for p-type conductivity, one of the native point defects, Zn vacancy (V_{Zn}), has received considerable attention because it has been believed that the dopant-V_{Zn} complex induced shallow acceptor level, such as Sb_{Zn}–$2V_{Zn}$, N_O–V_{Zn} [5, 6]. Besides, V_{Zn} acts as an acceptor with about 180 meV $\varepsilon(0/-)$ transition level in ZnO which has consistently predicted by first-principles investigation [4, 7–9]. Therefore, controllable incorporation of V_{Zn} could develop a significant way of achieving p-type ZnO in future.

Currently, there are some *ex-situ* methods for V_{Zn} creation, such as annealing in O_2 atmosphere, irradiation with high energy particles (electron, O-plasma), 193 nm excimer laser interactions [10–15]. However, V_{Zn} incorporation, during the growth, is critically required, which is very valuable and practicable for doping process [16, 17].

ZnO (0 0 0 1) surface has a net dipole moment in the repeat unit perpendicular to the surface which called 'Tasker-type 3' polar surfaces [18]. To make the infinite surface energy become finite, a counter field, caused by stoichiometric change or impurities adsorption, has to be introduced to conquer the dipole moment. Notably, the change of stoichiometric, such as missing or added atom during the growth, is one of the puzzles of the surface science. More specifically, a clean Zn-polar surface, consisted of Zn atoms with a dangling bond each, is unstable and prone to reconstructions. Previous investigations have noted that the high density triangular pits and islands are formed by removing Zn and O atoms on the Zn-polar surface bilayer [19, 20]. Theoretical calculations have revealed that there are several microscopic models of surface energy preferred reconstructions [21]. Among the different reconstruction models, the Zn-polar (0 0 0 1) (2 × 2) surface reconstruction with a single Zn atom vacancy per unit cell is very suitable for V_{Zn} controllable creation but hardly to been observed. According to the previous calculations, the (4 × 4) + Zn reconstruction surface, which was common reported in the growth of the Zn-polar ZnO films, has lower Madelung energy than the (2 × 2) configuration over a large range of not too oxygen-rich chemical surroundings [22].

Namely, a major question mark for the growth of (2 × 2) surface with a single Zn vacancy is extreme O-rich circumstances.

In the present letter, by using modulated metal epitaxy (MME), a dynamic molecular beam epitaxy (MBE) growth scheme [23], extreme O-rich chemical surrounding is obtained. Then, Zn vacancies in ZnO have been created via (2 × 2) surface reconstruction during the two-dimension epitaxy growth. *In situ* monitoring of the growth process using reflection high-energy electron diffraction (RHEED). In order to providing the direct evidence of (2 × 2) surface reconstruction with a single Zn vacancy, scanning tunneling microscopy (STM) has been employed. Variable-temperature/power steady-state photoluminescence (PL) spectroscopy is used to explain effects related to native point defects in ZnO.

2. Experimental details

A series of polarity-controlled ZnO films, under O-rich series, about 500 nm, were grown in DCA-P600 MBE system equipped with an oxford radio-frequency O_2 plasma source with ion removal control for active O, and solid-source effusion cells for Zn. Zn-polarity growth was realized by adjusting a 5 nm pre-epitaxial MgO buffer layer on 2 in. *c*-plane sapphire [24]. The growth temperature (T_g), 800 °C, was controlled by a contactless thermocouple placed behind the sapphire substrate. The background pressure depending on the O flux and the Zn cell corresponding beam equivalent pressures during growth were in the ranges $2 \times 10^{-6} - 5 \times 10^{-6}$ and 3.5×10^{-7} torr, respectively. The O_2 flow rate (in the ranges 1–3 sccm), controlled by a leak valve, and the plasma brightness, set at a higher level, were to ensure O-rich conditions for a rf power of 250 W. On the basis of Knudsen cosine law, MME growth, schematic drawing in figure 1, desynchronizes host epitaxy growth process from surface relaxation under extreme O-rich condition, allowing independent optimization by periodic Zn-shutter action. Considering the growth rate (2.4 nm min^{-1}), the Zn-shutter timing schedule was 40 s on and 20 s off.

3. Results and discussion

As shown in figure 2(a), a streaky RHEED patterns with intensity profiles along the [11–20] azimuths, indicating a well defined (4 × 4) reconstruction surface, is observed. With the O flux increasing, a bright (2 × 2) reconstructed surface with precise narrow and sharp reflexes evolves, figure 2(b). Both of these reconstructed surfaces are the fingerprint of Zn-polarity [22, 25, 26]. It is noteworthy that the RHEED patterns stay completely stable during the whole epitaxy growth process. The (2 × 2) reconstruction surfaces correspond to a unique surface stoichiometry, which means a single Zn vacancy created per unit cell on the surface. Further, these Zn vacancies, introduced by (2 × 2) reconstructed surface, will be partly occupied by another Zn atoms coming from the effusion source. Then, the minority of V_{Zn} were survived in the quantities of doping level, during the process of surface downward as inner layers of the film. In order to measure the

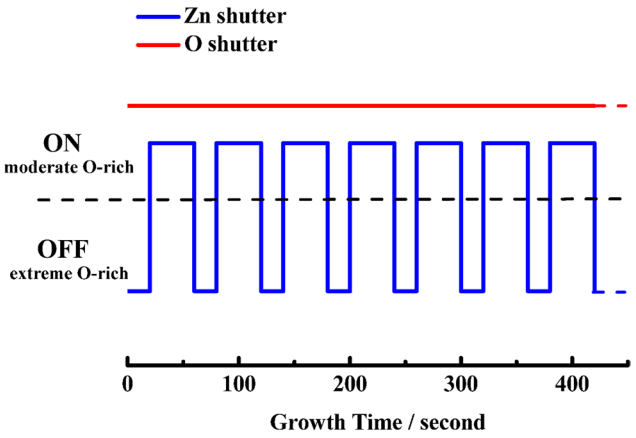

Figure 1. Schematic drawing of Zn, O fluxes versus time in modulated metal epitaxy. The extreme O-rich condition is obtained via periodic Zn-shutter action.

frozen in surface geometries obtained from the epitaxy growth conditions, the O shutter maintains open during the substrate temperature slowly decreasing, ensuring the extreme O-rich condition and thermodynamic equilibrium. Subsequently, the (2 × 2) reconstructed films have been transferred to the UHV chamber of STM. Figures 3(a) and (b) show STM images which were measured in the constant-current mode at tunneling currents of 0.03 to 0.02 nA and sample bias of 1.7 V. On the Zn-polarity face, as shown in figure 3(a), the surface sub-nanometer sized triangular pits and islands are formed by removing Zn atoms from the surface bilayer. It is suggested that the reduction of the surface Zn ratio results in a lower Madelung energy and a stabilized surface. From figure 3(b), the high resolution images, it can be identified clearly by atom sized cavities which indicating a single missing Zn atom [27, 28]. A line scan of the reconstructed surface, figure 3(d), indicates that the planar width of the pits is round 6 Å from hollow to hollow, which is very close to the double lattice constant ($a = 3.25$ Å). The measured pit depth is about 0.5 Å, which is underrated, due to the finite size of the STM tip apex.

To further investigate the point defects in the films, the steady-state PL spectra of all (2 × 2) reconstructed samples were excited by the cw He–Cd laser (excitation power 5 mW, emission line 325 nm). The PL signal was dispersed by a 0.5 m focal length monochromator with double 1200 groves mm^{-1} diffraction grating, which blazing wavelength were 300 nm and 500 nm, and detected with a semiconductor cooled charge-coupled device array. By using a closed-cycle helium refrigerator, variable-temperature PL were achieved in the range 12–300 K. A set of filters employed as an excitation power density (P_{exc}) adjuster. Figure 4(a) shows the PL spectra of the (2 × 2) reconstructed samples with three different O flux conditions at 12 K. In the part of ultraviolet range, the spectra of all samples present four dominant emission peaks at 3.360 eV, 3.344 eV, 3.310 eV and 3.227 eV, respectively. According to the previous studies and their energy values [29–31], the emission peaks, with photon energy decreasing, have been assigned to neutral donor-bound exciton (D^0,X), neutral acceptor-bound exciton (A^0,X), conduction band electrons to acceptors (e,A^0), donor-acceptor pair recombination (DAP). The free exciton

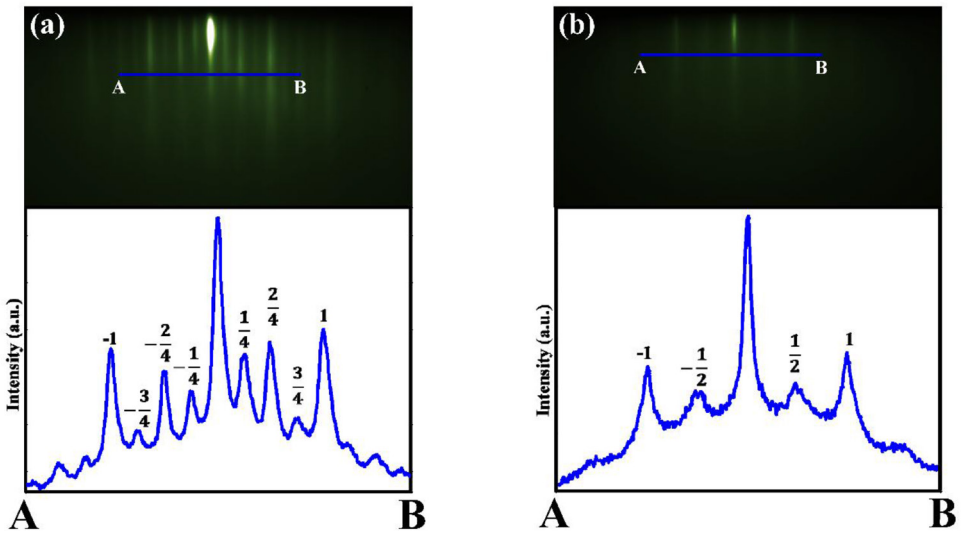

Figure 2. RHEED patterns and intensity profles along [11–20] electron beam azimuths show the (a) (4 × 4) and (b) (2 × 2) reconstructed ZnO surface with the O flux increasing. The sharp streaky RHEED patterns in both reconstructed surfaces can be clearly seen indicating the achievement of a flat ZnO surface morphology.

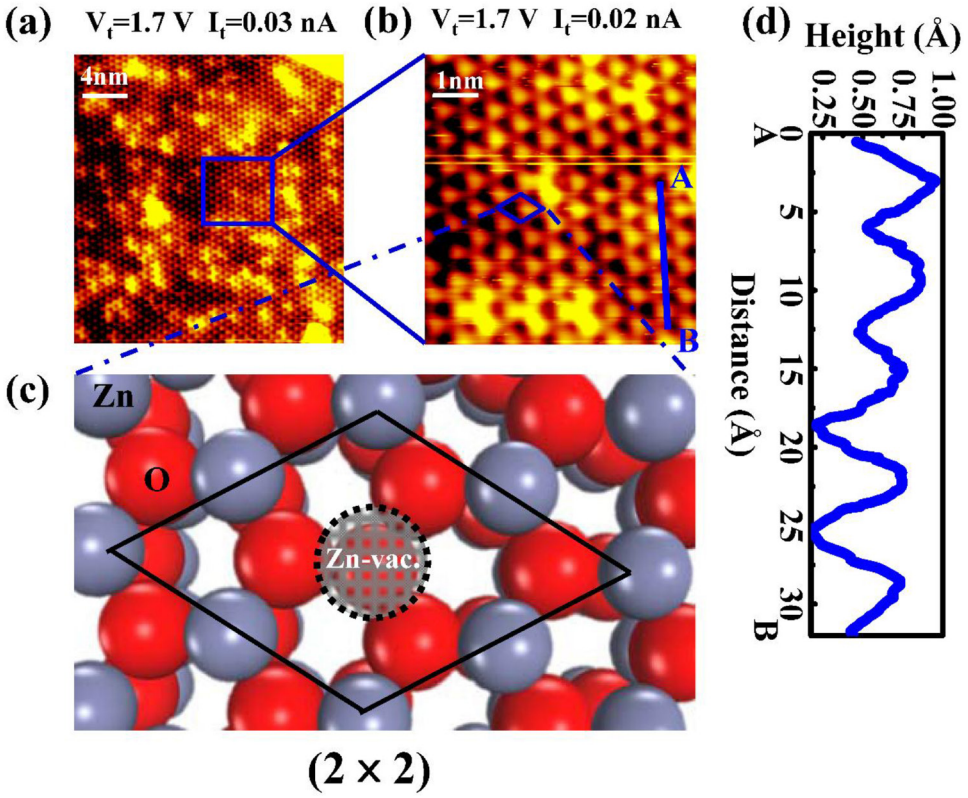

Figure 3. (a) High resolution STM image of the Zn-face. (b) Magnified view of the morphology of the triangular pit and island like those in (a). (c) Schematic diagram of (2 × 2) reconstruction with a single Zn vacancy. (d) Cross-section profile of the line shown in (b) indicating the planar width of the pits which is very close to the double lattice constant (a = 3.25 Å). The tunneling currents is 0.03 nA in (a) and 0.02 nA in (b) with sample bias of 1.7 V.

(FX) is also observed as a small peak located at about 3.374 eV. Two longitudinal optical (LO) phonon replicas of the DAP with a separation of ~73 meV, which consistent with the LO phonon energy in ZnO, are identified. As the previous pertinent reports, the present (e,A^0) located 3.310 eV is induced by basal plane stacking faults [3, 31]. Since the samples were unintentionally doped, the peak located at 3.344 eV is likely to be specifically associated with the V_{Zn} induced acceptor level. Note that deep level emission (DLE) in the visible spectral region shows significantly changes with the O flux increasing. There are two distinguished broad emission bands which maximum emission intensity at ~2.33 eV and ~1.76 eV, hereafter referred to as green luminescence (GL) and red luminescence (RL), respectively. The oxygen vacancy (V_O) related defects

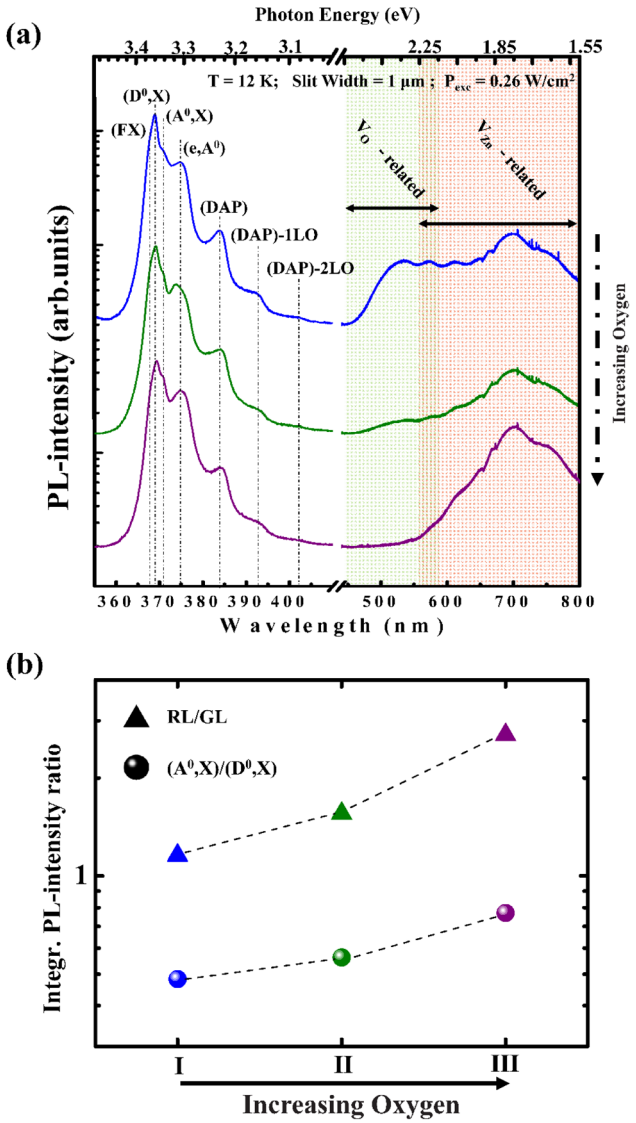

Figure 4. (a) PL of (2 × 2) reconstructed ZnO epilayers; (b) evolution of the integral PL-intensity ratio, RL/GL and $(A^0,X)/(D^0,X)$, with increasing O flux measured at $T = 12$ K.

are known to cause GL, in accordance with the majority of the relevant works (the exact peak position depends on defect concentration and on excitation intensity density), while RL associated with V_{Zn} related defects [10, 32, 33]. As unveiled in figure 4(b), the RL component is become dominating with the O flux increasing. The integral PL-intensity of (A^0,X) monotone improving, at the same time. This finding indicate that the samples, (2 × 2) surface reconstruction with a single Zn atom vacancy per unit cell, could manipulate the concentration of V_{Zn} by extreme O-rich condition realizing.

In order to supply additional evidence about the carrier recombination mechanisms, we have measured the variable-power PL spectroscopy. The PL spectra at 12 K and their evolution with increasing excitation power density from 0.02 to 0.26 W cm^{-2} for RL dominated sample are shown in figure 5(a). Interestingly, the position and shape of the RL do not change with excitation intensity density changing, which

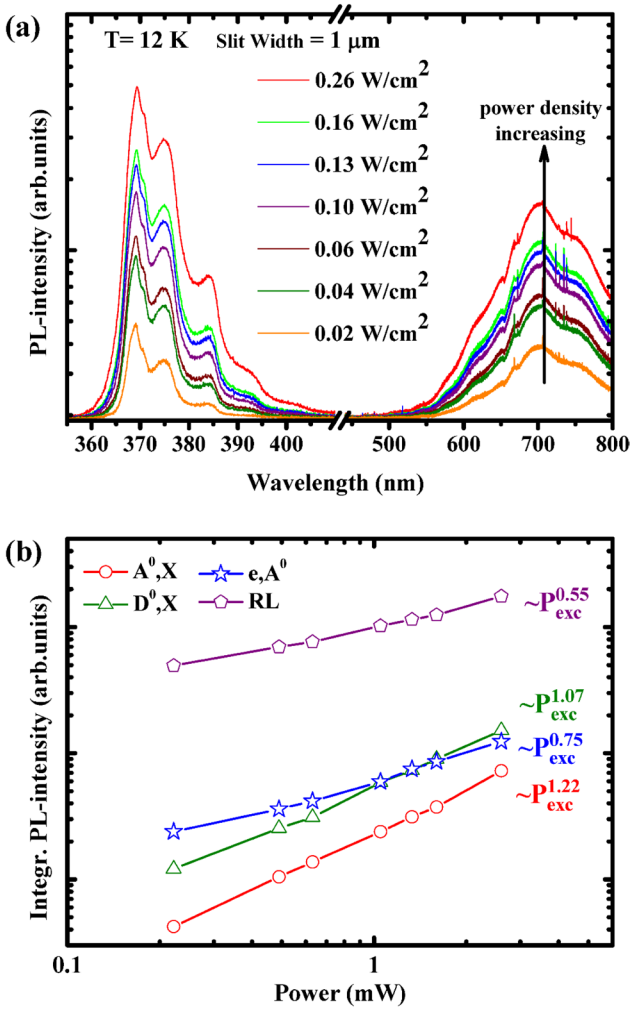

Figure 5. (a) Excitation power-dependent PL measurements of (2 × 2) reconstructed ZnO film at 12 K; (b) log–log plot of integral PL-intensity as a function of excitation power. Power-law show different P_{exc} dependencies.

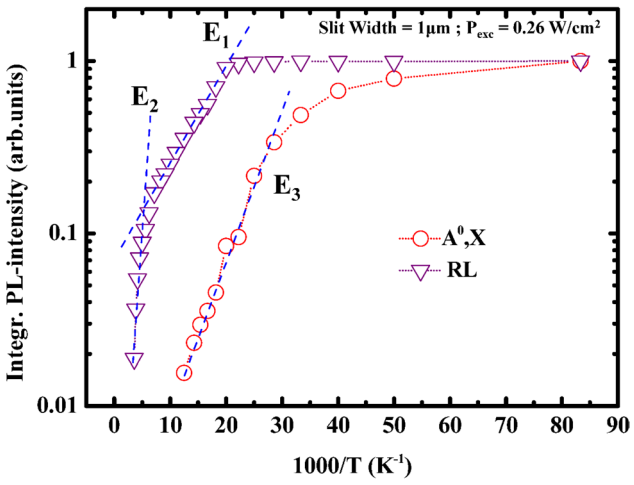

Figure 6. Temperature dependencies of the normalized integral PL-intensity at RL band and (A^0,X) emission under a selected excitation power density. The dashed line is calculated by using equation (1).

suggesting that the RL band is originated from an internal transition in the V_{Zn} defect, since the internal transitions free from the effect of potential fluctuations [34]. Figure 5(b) shows excitation power dependence of the integral PL intensity for (A^0,X), (D^0,X), (e,A^0) and RL, extracted from figure 5(a). By using power-law model $I_{PL} \sim (P_{exc})^k$, where I_{PL} is the integral PL intensity, P_{exc} is excitation intensity, the power factor k is fitted very well with each recombination mechanisms, according to the previous studies, which means the k for (A^0,X) and (D^0,X) is in the range $1 < k < 2$ while for (e,A^0) and RL is in the range $0 < k < 1$ [35, 36].

As observed in the low temperature PL spectrum, the two emission peaks, (A^0,X) and RL, are probably both associated with V_{Zn}. Figure 6 shows the integral PL intensity of the (A^0,X) and RL as a function of the 1000/T, in which both emissions exhibit the thermal quenching. The integral PL intensity decreasing can be described by the following expression:

$$I(T) = I_0/[1 + C\exp(-E_a/k_B T)] \quad (1)$$

where E_a is usually elucidated as some activation energy, C is a fitting constant, and I_0 is the integral PL intensity at $T = 0$. By fitting the experimental data with equation (1), the Arrhenius plots were presented in figure 6. The RL band presents two slopes which indicating there are two distinct thermal quenching mechanisms dominated in different temperature range. For the first part, the quenching start from ~50 K with the localization energy (E_1) of ~12.8 meV which suggesting a participation of thermal delocalization of shallow donor-bound exciton getting involved in radiative recombination with deep V_{Zn} acceptor centers [33]. To the temperature range $T > 200$ K, the activation energy (E_2) was fitted to be ~95 meV. This performance of quenching, starting at higher temperatures and having a steeper slope, indicates PL via deeper defects, which can be explained by Seitz–Mott mechanism [37]. In the meantime, we obtain the localization energy of (A^0,X), E_3, is about 45.5 meV. With the purpose of calculate the acceptor binding energy E_A, the empirical Haynes rule [38],which described by $E_a = \alpha E_A + \beta$, has been applied. Different from donor-bound exciton in ZnO, the coefficients is $\alpha = 0.24$ and $\beta = -0.02$, for acceptor-bound exciton, according to a very comprehensive study [39]. We estimate the E_A, for the 3.344 eV emission, to be about 189 meV, which is very close to the first-principles investigation for V_{Zn} acceptor level.

Conclusions

In summary, we developed a practicable way to manipulation of V_{Zn} in ZnO via Zn-polar surface (2 × 2) reconstruction. Combined *in situ* RHEED, STM, and Variable-temperature/power steady-state PL studies reveal that the V_{Zn} defects have been produced, effectively. During the whole epitaxy growth process, the (2 × 2) reconstruction surfaces stay completely stable in extreme O-rich conditions, according to the monitoring of RHEED patterns. From high resolution STM images, the atom sized triangular pit and island have been observed which indicating (2 × 2) reconstructed surface with a single missing Zn atom. The emissions related to V_{Zn}, (A^0,X) at 3.344 eV and RL bands ~1.76 eV, have been detected by the temperature-dependent PL measurement. The acceptor binding energy for the 3.344 eV emission was estimated about 189 meV, which is in good agreement with theory results.

Acknowledgments

The authors gratefully acknowledge support from the National Natural Science Foundation of China (NSFC) under Grant No. 61376054 and 61505200.

References

[1] Özgür Ü, Alivov Ya I, Liu C, Teke A, Reshchikov M A, Doğan S, Avrutin V, Cho S-J and Morkoç H 2005 *J. Appl. Phys.* **98** 041301
[2] Service R F 1997 *Science* **276** 895
[3] McCluskey M D and Jokela S J 2009 *J. Appl. Phys.* **106** 071101
[4] Janotti A and Van de Walle C G 2007 *Phys. Rev.* B **76** 165202
[5] Przeździecka E, Kamińska E, Pasternak I, Piotrowska A and Kossut J 2007 *Phys. Rev.* B **76** 193303
[6] Liu L *et al* 2012 *Phys. Rev. Lett.* **108** 215501
[7] Kohan A, Ceder G, Morgan D and Van de Walle C 2000 *Phys. Rev.* B **61** 15019
[8] Zhang S B, Wei S H and Zunger A 2001 *Phys. Rev.* B **63** 075205
[9] Puchala B and Morgan D 2012 *Phys. Rev.* B **85** 195207
[10] Dong Y F, Tuomisto F, Svensson B G, Kuznetsov A Y and Brillson L J 2010 *Phys. Rev.* B **81** 081201
[11] Børseth T M, Svensson B G, Kuznetsov A Y, Klason P, Zhao Q X and Willander M 2006 *Appl. Phys. Lett.* **89** 262112
[12] Khan E H 2014 *J. Appl. Phys.* **115** 013101
[13] Khan E H, Weber M W and McCluskey M D 2013 *Phys. Rev. Lett.* **111** 017401
[14] Zubiaga A, Tuomisto F, Coleman V A, Tan H H, Jagadish C, Koike K, Sasa S, Inoue M and Yano M 2008 *Phys. Rev.* B **78** 035125
[15] Børseth T M, Tuomisto F, Christensen J S, Monakhov E V, Svensson B G and Kuznetsov A Y 2008 *Phys. Rev.* B **77** 045204
[16] Reynolds J G, Reynolds C L Jr, Mohanta A, Muth J F, Rowe J E, Everitt H O and Aspnes D E 2013 *Appl. Phys. Lett.* **102** 152114
[17] Amini M N, Saniz R, Lamoen D and Partoens B 2015 *Phys. Chem. Chem. Phys.* **17** 5485
[18] Tasker P W 1979 *J. Phys.* C **12** 4977
[19] Kresse G, Dulub O and Diebold U 2003 *Phys. Rev.* B **68** 245409
[20] Dulub O, Diebold U and Kresse G 2003 *Phys. Rev. Lett.* **90** 016102
[21] Valtiner M, Todorova M, Grundmeier G and Neugebauer J 2009 *Phys. Rev. Lett.* **103** 065502
[22] Pal S, Jasper-Tönnies T, Hack M and Pehlke E 2013 *Phys. Rev.* B **87** 085445
[23] Zhong M, Roberts J, Kong W, Brown A S and Steckl A J 2014 *Appl. Phys. Lett.* **104** 012108
[24] Kato H, Miyamoto K, Sano M and Yao T 2004 *Appl. Phys. Lett.* **84** 4562
[25] Mei Z X, Du X L, Wang Y, Ying M J, Zeng Z Q, Zheng H, Jia J F, Xue Q K and Zhang Z 2005 *Appl. Phys. Lett.* **86** 112111
[26] Du M H, Zhang S B, Northrup J E and Erwin S C 2008 *Phys. Rev.* B **78** 155424

[27] Xu H, Dong L, Shi X Q, Van Hove M A, Ho W K, Lin N, Wu H S and Tong S Y 2014 *Phys. Rev.* B **89** 235403
[28] Lai J H, Su S H, Chen H-H, Huang J C A and Wu C-L 2010 *Phys. Rev.* B **82** 155406
[29] Teke A, Özgür Ü, Dogan S, Gu X, Morkoç H, Nemeth B, Nause J and Everitt H O 2004 *Phys. Rev.* B **70** 195207
[30] Wagner M R *et al* 2011 *Phys. Rev.* B **84** 035313
[31] Schirra M, Schneider R, Reiser A, Prinz G M, Feneberg M, Biskupek J, Kaiser U, Krill C E, Thonke K and Sauer R 2008 *Phys. Rev.* B **77** 125215
[32] Sann J, Stehr J, Hofstaetter A, Hofmann D M, Neumann A, Lerch M, Haboeck U, Hoffmann A and Thomsen C 2007 *Phys. Rev.* B **76** 195203
[33] Knutsen K E, Galeckas A, Zubiaga A, Tuomisto F, Farlow G C, Svensson B G and Kuznetsov A Y 2012 *Phys. Rev.* B **86** 121203
[34] Reshchikov M A, Demchenko D O, McNamara J D, Fernández-Garrido S and Calarco R 2014 *Phys. Rev.* B **90** 035207
[35] Fonoberov V A, Alim K A, Balandin A A, Xiu F and Liu J 2006 *Phys. Rev.* B **73** 165317
[36] Ton-That C, Weston L and Phillips M R 2012 *Phys. Rev.* B **86** 115205
[37] Reshchikov M A 2014 *J. Appl. Phys.* **115** 012010
[38] Haynes J R 1960 *Phys. Rev. Lett.* **4** 361
[39] Gutowski J, Presser N and Broser I 1988 *Phys. Rev.* B **38** 9746